Article:

Ni, J. and Rockett, P.I. (2014) Tikhonov Regularization as a Complexity Measure in Multiobjective Genetic Programming. IEEE Transactions on Evolutionary Computation, 19 (2). 157 - 166. ISSN 1089-778X

https://doi.org/10.1109/TEVC.2014.2306994

Genetic Programming and Evolvable Machines manuscript No.
(will be inserted by the editor)

Training Genetic Programming Classifiers by Vicinal-Risk Minimization

Ji Ni · **Peter Rockett**

Received: May 13, 2014/ Accepted: ???

Abstract We propose and motivate the use of vicinal-risk minimization (VRM) for training genetic programming classifiers. We demonstrate that VRM has a number of attractive properties and demonstrate that it has a better correlation with generalization error compared to empirical risk minimization so is more likely to lead to better generalization performance, in general. From the results of statistical tests over a range of real and synthetic datasets, we further demonstrate that VRM yields consistently superior generalization errors compared to conventional empirical risk minimization.

Keywords Genetic programming · Classification · Vicinal-risk minimization

1 Introduction

Classification [8] is one of the most important tasks in machine learning and aims to discover a discriminating function that maps an N-dimensional input vector, $\mathbf{x} \in \mathbb{R}^N$ to a label, $y \in \{-1,+1\}$; without loss of generality we consider only binary, or two-class, classification in this paper. Empirical learning is ill-posed [4,25], which means that classifiers trained by minimizing the empirical risk (i.e, the fraction of misclassified training patterns) can exhibit a range of generalization errors over unseen test data. This ill-posedness is particularly acute for small datasets; it is the case of small datasets that we *explicitly* address in this paper. For some given size of training set, there is a trade-off between the empirical risk and the *complexity* of the discriminating function [4]. Overly simple functions lack sufficient flexibility to capture the

J. Ni
Department of Electronic and Electrical Engineering, University of Sheffield, Mappin Street, Sheffield, S1 3JD, UK
E-mail: j.ni@outlook.com

P. Rockett
Department of Electronic and Electrical Engineering, University of Sheffield, Mappin Street, Sheffield, S1 3JD, UK
E-mail: p.rockett@sheffield.ac.uk

class concepts, have a large training error and underfit. At the other extreme, overly complex functions produce decision surfaces with low – possibly zero – training error but which overfit the training set. Both extremes – underfitting and overfitting – yield large generalization errors over independent test data. In general, there exists some 'optimal' model complexity between underfitting and overfitting although addressing this *model selection* problem is often challenging. One of the great strengths of genetic programming (GP) for the empirical modeling of data is that the complexity of the function can evolve to match the data at hand. Nonetheless, the loss function on which a GP classifier is trained plays a pivotal role.

A straightforward illustration of the deficiencies of empirical risk minimization (ERM) is shown in Figure 1 where a small training set of non-separable data is assumed drawn from two, arbitrary, two-dimensional class distributions, also shown. The training data are separated by two arbitrary candidate decision surfaces, g_1 and g_2.

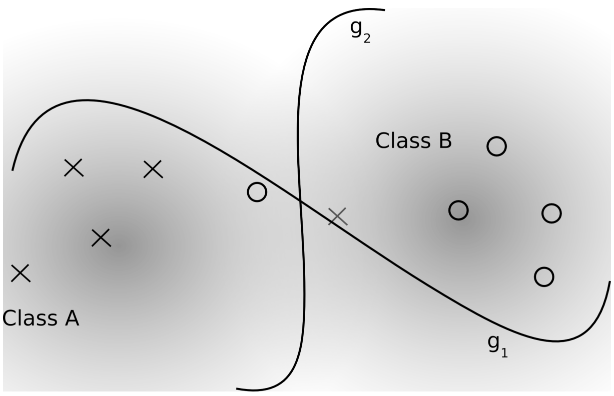

Fig. 1 Illustration of the deficiency of 0/1 loss. A small training set, shown as crosses and circles have been drawn from the distributions of class A and B, respectively. g_1 and g_2 are two arbitrary, candidate decision surfaces.

As gauged by the empirical risk, g_1 and g_2 give identical values because both misclassify two training set patterns out of ten. There is no reason to prefer one decision surface over another; more generally, *any* function which misclassifies *any* two training patterns cannot be set apart from g_1 and g_2 by ERM. As to the generalization abilities of g_1 and g_2, it is clear that g_1 will exhibit a worse test error than g_2 since it does a worse job of separating the two underlying class distributions although this, of course, cannot be judged by ERM over this training set. Note that this problem is nothing to do with under- or overfitting, but rather, a fundamental limitation of empirical risk. In summary, it is clear that the same value of empirical risk can produce a range of possible generalization errors – it is, of course, the objective of machine learning to produce the best possible generalization error. It is noteworthy that almost all GP classifiers reported in the literature have involved minimizing empirical risk.

In order to attempt to strike a balance between error over the training set and the complexity of the discriminant, a number of methods have been employed in the machine learning field. Classically, *regularization* [24] seeks to minimize the weighted sum of a risk functional and some measure of discriminant complexity although how to decide on the weighting (the so-called regularization constant) between the two terms usually involves cross-validation [4]. The parsimony principle [18] much-used in GP is an example of regularization. Minimum description length (MDL) approaches [20] can also be viewed as regularization. Iba et al. [13] attempted to apply MDL to GP but failed to account for the not-necessarily-minimal form of the trees – logically, MDL can only be applied to trees which have been simplified to truly minimal algebraic form which, we suspect, is an NP-complete task. In Bayesian approaches, the log prior can be interpreted as a regularization term [25].

Over the past twenty years, the structural risk minimization (SRM) framework of Vapnik [25] has been a dominant paradigm in machine learning and has lead to the powerful notion of maximum margin classification as well as support-vector machines (SVMs). Application of SRM to genetic programming classifiers, however, is technically difficult. Borges et al. [2] interpreted the number of multiplication and division nodes in GP trees as the Vapnik-Chervonenkis (VC) dimension of their discriminant function and claimed to apply SRM principles to GP training although they offered no theoretical justification as to why this quantity is connected to the shattering dimension [4] of the function. The fact that these authors were able to observe improved performance was probably because their “VC dimension” was employed in a conventional regularization framework and the value of the regularization constant tuned to yield improved performance over non-regularized comparators. Amil et al. [1] derived an expression for the VC dimension of a GP tree proportional to the upper bound on the number of nodes in the tree (assuming no exponential function nodes) although the tightness of this bound, and therefore its adequacy for SRM, is unknown [11].

Exploring the complexity of the discriminant implemented by a GP tree is feasible using multiobjective (MO) [27] (or other parsimony) methods by simultaneously minimizing the empirical error/complexity leading to a (Pareto) set of solutions which delineate this trade-off. The problem remains, as we have argued above, that minimizing the empirical risk over a training set does not necessarily equate to minimizing the generalization error of the resulting classifier. The fact that the empirical risk over a training-set is a one-to-many mapping to test error undermines the validity of the regularization framework, especially under the small sample conditions that we are expressly addressing here. For this reason we have explored the use of an improved loss function for training GP classifiers.

Although SRM principles are not straightforward to apply in GP, Vapnik [25] has also presented vicinal-risk minimization (VRM), a framework complementary to SRM; in some cases VRM and more conventional SRM approaches can be shown to yield identical results [25]. Crucially in the present context, applying VRM in GP is readily tractable. We introduce VRM in Section 2. We describe our experimental setup in Section 3 and report the results of statistical comparisons over a range of real and synthetic datasets in Section 4 with statistically-founded evidence that VRM produces superior classifiers. We discuss a number of aspects of VRM in Section 5 before summarizing the paper in Section 6.

2 Vicinal Risk

Given some set of ℓ training data drawn independent and identically-distributed (iid) from a data distribution $P(\mathbf{x}, y)$:

$$\mathscr{D} = \{\mathbf{x}_1 \to y_1, \mathbf{x}_2 \to y_2, \ldots \mathbf{x}_\ell \to y_\ell\}$$

where $\mathbf{x}_i \in \mathbb{R}^N$ and $y \in \{-1, +1\}$, the task of training a *scoring* classifier in machine learning is to select some discriminative function $f(\mathbf{x})$ such that:

$$f(\mathbf{x}) \begin{cases} < 0 & \text{Predict class `-1'} \\ \geq 0 & \text{Predict class `+1'} \end{cases} \tag{1}$$

We require to select the $f(\mathbf{x})$ which minimizes the expected risk, $R(f)$ which will ensure optimum generalization over future unseen examples drawn from $P(\mathbf{x}, y)$:

$$R(f) = \int L[f(\mathbf{x}), y] \, dP(\mathbf{x}, y) \tag{2}$$

where L is some loss function. Unfortunately, $P(\mathbf{x}, y)$ is not known in practice and so a conventional approximation has been to minimize the *empirical* risk, R_{emp} (i.e., the expectation of 0/1 loss) over the training set. We take the loss function to be:

$$L[f(\mathbf{x}), y] = H[-yf(\mathbf{x})] \tag{3}$$

where $H()$ is the Heaviside step function. Thus for $\mathbf{x}$-values which would give rise to a misclassification, (3) is unity; conversely, for $\mathbf{x}$-values which yield correct classification, the loss is zero. Thus R_{emp} can be formally defined as:

$$R_{emp}(f) = \frac{1}{\ell} \sum_{i=1}^{\ell} H[-y_i f(\mathbf{x}_i)] \tag{4}$$

As is clear from the above, the fundamental shortcoming of the 0/1 loss is due to its discrete nature, in particular, that a pattern is either classified correctly, in which case it contributes zero to the cumulative loss, or the pattern is misclassified and so contributes unity to the loss. Crucially, no account is taken of the *margin* by which a pattern is misclassified (or indeed, correctly classified). A misclassified pattern which is just the wrong side of a decision surface is weighted equally with a pattern that is a very large distance from the decision surface; intuitively, the latter case should be treated as more serious than the former. As a logical consequence, a pattern's distance from the decision surface should weight its contribution to the loss[1].

Vapnik [25] has motivated *vicinal risk* by assuming that the (unknown) data distribution is locally 'smooth' in which case $P(\mathbf{x}, y)$ can be approximated by placing a *vicinity function* on each training datum – this process can be thought of as either resampling or, equivalently, interpolating $\mathscr{D}$. Since the shortcomings of 0/1 loss are due to its discrete nature, smoothing the training set will have the effect of stabilizing the training process. Vapnik [25] described two possible types of vicinity functions,

[1] This is exactly what is done in the hinge loss used in soft-margin support-vector machines [4].

hard and *soft*. Hard vicinity functions have an abrupt cutoff at some distance from a training datum – under a 2-norm, this would be a ball or hypersphere centered on each datum. Whereas a hard vicinity function has a constant, non-zero value up to the cutoff distance and zero beyond, a soft vicinity function, such as a Gaussian kernel, typically has a peak value at the training datum and a monotonically-reducing value with increasing distance from the datum. Entirely equivalently, placing a kernel over each training datum can be viewed as approximating $P(\mathbf{x}, y)$ using a Parzen windows density estimator [3,8] for which a Gaussian kernel is a natural choice[2]. Here we develop the soft vicinity function approach because: i) it is more tolerant of the setting of scale of the kernel and ii) there is a technical requirement with hard vicinity functions that they do not overlap in pattern space [25].

Taking the loss function given in (3), analogous to minimizing (2), we wish to select the f which minimizes the vicinal risk, R_{VR} which is the expectation of (3) over the data distribution. Writing the necessary risk functional in a somewhat different form to Vapnik:

$$R_{\mathrm{VR}}(f) = \int L[f(\mathbf{x}), y]\, dP(\mathbf{x}, y) \tag{5}$$

$$\approx \frac{1}{\ell} \sum_{i=1}^{\ell} \int H[-y_i f(\mathbf{x})]\, G(\mathbf{x}|\mathbf{x}_i, \sigma_i^2) d\mathbf{x} \tag{6}$$

where $G()$ is the Gaussian kernel of variance σ_i^2 placed on the i-th datum, and $P(\mathbf{x}, y)$ is approximated by the Parzen windows estimate of a sum of Gaussians. The integral within (6) has a straightforward interpretation as the hypervolume, in the N-dimensional pattern space, of the portion of the i-th kernel which falls on the 'wrong' side of the decision surface and hence would give rise to misclassification.

A number of properties of VRM is apparent:

- Under VRM, we seek to minimize a continuous function (6), thereby removing the problem with 0/1 loss of being discrete. Patterns contribute to the loss depending on their distance from the decision surface, or more strictly, the hypervolume of the kernel function falling on the 'wrong' side of the decision surface. It is clear that correctly-classified patterns a long way from the decision surface will make a very small contribution to the loss and will hence have a minimal influence on the placement of the decision surface – this is highly desirable since only data in the vicinity of the decision surface run the risk of misclassification and should 'negotiate' the location of the decision surface.
- At distances greater than $\simeq 3\sigma$ from the decision surface, the contribution to the loss of an incorrectly-labeled datum saturates at unity, conferring robustness to outliers.
- As $\sigma^2 \to 0$, the Gaussian kernel in (6) tends to a δ-function and so the vicinal risk tends to the empirical risk in (4). Thus empirical risk can be understood as a special case of vicinal risk.

[2] We omit the normalization of the Parzen density estimate since this contributes only a multiplicative constant that does not affect the subsequent minimization stage.

– As $\sigma^2 \to \infty$, the value of risk (6) tends to 0.5 since in the limit, 'half' the kernel extends either side of the decision surface.
– σ^2 defines a characteristic 'scale' for the learning problem which will vary by dataset.

Chapelle et al. [3] have directly minimized VRM for linear classifiers, assigning each training datum kernel its own value of σ_i^2 proportional to a measure of local density although the constant of proportionality had to be determined by cross-validation. As far as we are aware, the present paper is the first report of applying VRM to genetic programming classifiers.

Key to the computational tractability of VRM in genetic programming is the evaluation of the integral in (6). Rather than the inconvenient evaluation of an N-dimensional integral, we can propagate the Gaussian kernel on the i-th pattern through into the 1D decision space, the image of $f(\mathbf{x})$. This yields a distribution $p_i(z)$ in the 1D decision space, z as shown in Figure 2. Notice that because the mapping implemented by a GP tree will, in general, be non-linear, $p_i(z)$ will be not generally be a Gaussian distribution despite the samples being Gaussian-distributed about $\mathbf{x}_i$ in pattern space. Equation (6) for the vicinal risk can be rewritten as:

$$R_{\mathrm{VR}} \approx \frac{1}{\ell} \sum_{i=1}^{\ell} \int H[-y_i \times z]\, p_i(z) dz \tag{7}$$

Notice that the integrals under the summations in both (6) and (7) evaluate the probability of a point drawn from $G(\mathbf{x}|\mathbf{x}_i, \sigma_i^2)$ being misclassified. To approximate the integral in (7) we can conveniently use Monte Carlo integration [21] whereby for the i-th pattern, we draw q_i samples from the Gaussian distribution $G(\mathbf{x}|\mathbf{x}_i, \sigma_i^2)$, and propagate each resulting vector through f to yield a corresponding set of scalar values of z. Counting the number of values of z which predict the incorrect class according to (1) for the i-th training pattern, and dividing by q_i approximates the value of the integral for the i-th pattern in (7); evaluating an integral by Monte Carlo in 1D is much more efficient than performing the same evaluation in N dimensions, particularly when N is large [21]. The probability of misclassification for the i-th pattern is illustrated by the shaded region in Figure 2. It is the expectation of this probability over the training set that we seek to minimize which is achieved by taking the expectation over the integrals (i.e. averaging) in (7).

We can conveniently organize the Monte Carlo integration and the calculation of (7) by taking q pre-calculated samples at each training datum and storing the results as an augmented training set. The value of vicinal risk is thus approximated by the total number of misclassified training patterns divided by $\ell \times q$. The mechanics of calculating vicinal risk are thus identical to calculating empirical risk, except over an augmented training set.

Ultimately, we desire a loss function which is more predictive of (i.e. better correlated with) test error than empirical risk which is a one-to-many mapping. Namely, minimizing a given risk functional will produce a classifier with superior generalization performance. We have explored this issue in Section 4.1 where we present results that demonstrate that vicinal risk does indeed have this key property of supe-

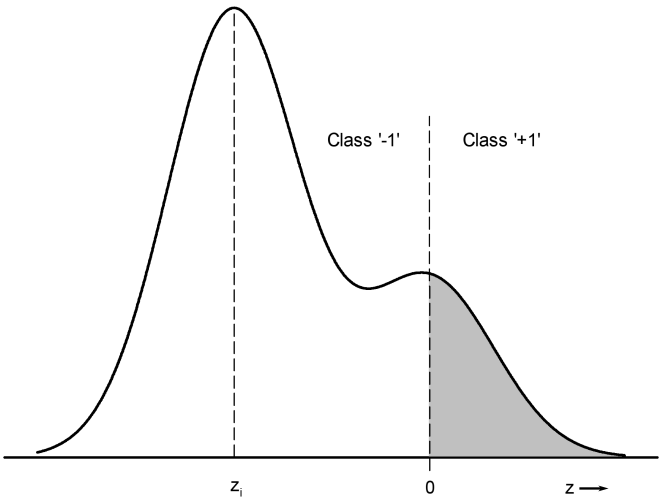

Fig. 2 Illustration of the propagation of the Gaussian kernel from pattern space into decision space. The shaded area is the probability of misclassification of the pattern at $\mathbf{x}_i$ which projects to z_i in decision space.

rior correlation with test error. In Section 4.2 we show that it yields statistically lower generalization errors over a range of datasets.

3 Experimental Setup

3.1 GP Configuration

We have used conventional tree-based GP to train discriminant functions where each individual in the population represents a function $y = g(\mathbf{x}) = f(\mathbf{x}) - t$, where t is a threshold. We find that learning a discriminant in this more flexible form is easier than trying to evolve f directly with an implicit zero threshold. In the process of evaluating the fitness of an individual, we run a further search for the threshold t using *golden section search* (GSS) [17] in the 1D decision space to yield the lowest training set error (either empirical or vicinal risk). Despite the fast convergence of GSS, there is an assumption that the function is continuous and unimodal, which is not necessarily satisfied here. To make the search for t robust, we divide the whole decision space into multiple intervals and perform GSS within each to reduce the risk of the algorithm getting stuck in a local optimum; five intervals appears to give a satisfactory compromise between speed and robustness of the search.

We have employed the Pareto-Converging Genetic Programming (PCGP) GP-variant of the multiobjective, steady-state Pareto-converging algorithm [15] to compare empirical risk (ER) and vicinal risk (VR). PCGP has been shown to out-perform other contemporary MOGP algorithms in a comparative study [26]. In PCGP, two parents are selected from the population using stochastic, rank-based selection, and bred by crossover and mutation to produce two offspring which are appended to the population. The population is then re-ranked, and the weakest two members of the current population discarded; the process is then repeated. In the PCGP algorithm, crossover and mutation are always applied. See [15,27] for further details.

In MOGP, the risk – either empirical or vicinal – was one objective, and node count, a straightforward measure of syntactic tree complexity, was the other. We have used multiobjective GP here specifically to explore the trade-off between training error and a measure of model complexity (node count). Although MO methods were originally motivated by the desire to control bloat – see, for example, [9] – MO approaches actually *minimize* tree size (for some given value of the other objective, typically error), yielding the set of the most parsimonious models. What emerges from MOGP is a Pareto set of equivalent, non-dominated solutions which samples this trade-off although the individual which yields the best generalization typically needs to be determined by an independent model-selection step (see Section 3.3). Conventional bloat control has operated by limiting tree growth, whereas MOGP seeks to minimize tree size for some given error. The two are profoundly different outcomes. Thus MO methods perform highly- effective bloat control almost as a side-effect of minimizing tree size. Silva et al. [22] have observed that overfitting and bloat can occur independently, reinforcing the point that simply preventing excessive growth in tree size does not necessarily control the *complexity* of the generated mapping, $\mathbf{x} \to y$.

The parameters used in the experimental work are listed in Table 1.

To calculate the vicinal risk of a GP tree by Monte Carlo integration, we have used 200 samples per training datum drawn from the Gaussian kernel placed over each datum, pre-calculated and stored as an augmented training set.

Table 1 GP Parameters Used

Population size	100
Population initialization	Ramped half-and-half [18]
No. of tree evaluations	10,000
Crossover	Point crossover [18]
Mutation	Point mutation [18]
	with tree depth = 4
Node types	Unary minus
	Addition
	Subtraction
	Multiplication
	Protected division
Terminal nodes	Pattern attributes
	Constants $\in [0, 0.01, 0.02..., 0.99]$

3.2 Datasets

We have conducted experiments with a range of synthetic and real 2-class datasets. We have used three synthetic datasets: a 2D mixture of Gaussians due to Ripley [19], a second 2D mixture of Gaussians due to Hastie et al. [11], and a 10D Gaussian problem with class-mean vectors of $(0, \ldots 0)$ and $(1/\sqrt{10}, \ldots 1/\sqrt{10})$ and equal, unit covariance matrices. The Ripley and Hastie datasets have very non-linear optimal decision boundaries. For these synthetic problems, we randomly drew 100 patterns of each class to produce datasets of 200 data which were randomly partitioned into training and test partitions.

In addition to the three synthetic datasets described above, we also used eight real datasets from UCI Repository [10] to compare the performance of ERM and VRM; the validity of using the UCI datasets has been established by Soares [23]. Details of the datasets are summarized in Table 2. Most have real attributes since the formulation of VRM implicitly makes this assumption although some datasets also contain categorical attributes which we have mapped to integers in the order in which they are described in the UCI documentation. 2Glass is a 2-class dataset generated from the original 6-class UCI dataset to classify float and non-float glasses. The Pima Indians Diabetes dataset is the version due to Ripley[3] with the incomplete/implausible records removed.

Table 2 Details of Datasets

Name	Dimensionality	#Patterns
2-Glass	9	163
BUPA	6	345
Pima Indians Diabetes (PID)	7	532
German Credit	24	1000
Australian Credit	14	690
Statlog Heart	13	270
Wisconsin Breast Cancer (WBC)	9	683
Wisconsin Diagnostic Breast Cancer (WDBC)	30	569
Ripley [19]	2	200
Hastie [11]	2	200
10D-Gaussian (10D-G)	10	200

3.3 Testing Methodology

To gauge the statistical significance of the results, we have used the Wilcoxon two-sided non-parametric test [7], comparing the pairs of test error estimates resulting from each training partition for empirical and vicinal risks. Although lacking the power of parametric tests, Demšar [7] points-out that the necessary assumptions required by parametric tests are typically violated in machine-learning situations, and so the Wilcoxon test is preferred; see [7] for further details. We have performed the Wilcoxon test by making fifteen [16] random splits of each dataset into equal-sized partitions, using one as a training set and the other as a test set.

In order to allow for the stochastic nature of GP, the estimate of test error for every split was taken as the median of 30 runs (i.e., a total of $15 \times 30 = 450$ runs per dataset) with an independently-generated initial population for each run. The single individual selected from each MOGP run for inclusion in the statistical analysis was the individual in the final population with either:

[3] Downloadable from `http://www.stats.ox.ac.uk/pub/PRNN/`.

– The smallest training error over the whole (final) population.

OR

– The smallest error over the test partition from the Pareto front.

We have included individuals with the smallest training error since these are what would be used in a single objective GP method and thus allow comparison with our MOGP approach.

Ideally, the training, validation and test procedures should all be conducted with three disjoint partitions of the dataset [11] although in practice, the the limited size of many datasets dictates a more pragmatic approach. Considering the typical procedure used in single-objective GP (SOGP), an investigator would perform multiple, often 30, GP runs each with independently-generated initial populations and report the best test error over the multiple runs. Each of this sequence of SOGP runs would return a candidate model (i.e. a hypothesis) so the process of selecting the hypothesis with the smallest error is actually a *model selection* procedure. Our model selection procedure is thus entirely equivalent to that typically used in SOGP apart from the (immaterial) means by which the candidate hypotheses are generated: the Pareto set of candidates obtained from a single MOGP run, or thirty candidates, one obtained from each of a sequence of thirty SOGP runs. We prefer MOGP because the candidate set spans the range of model complexities from low to high, which cannot be guaranteed by independent SOGP runs.

In addition, the estimate of test error for a given individual is a single realization of a random variate so in order to mitigate the chance of this single 'draw' coming from the low-error extreme of the error distribution, it is desirable to make the standard error of the estimate as small as possible. This has dictated our use of half of the data for the test partition since the standard error falls as a square root of the test set size.

For each dataset, we have used a single, optimized value of σ^2 for every smoothing kernel determined using the procedure outlined in Section 4.1. To facilitate a single value of σ^2 on each dimension, we normalized each attribute to unit variance over every training partition and then normalized the test partition using the same scaling. Chapelle et al. [3] assigned individually-optimized values of σ^2 to each training datum although we have adopted a simpler strategy here; potentially individually-assigned values of σ^2 may improve the performance of VRM by producing a locally-smoother approximation to $P(\mathbf{x}, y)$.

4 Results

4.1 Correlation with Test Error

To explore whether VRM exhibits superior correlation between training and test errors than ERM, we have sampled a large number of randomly-initialized, partially-trained and fully-trained GP trees. We present typical results for the Hastie dataset where we have accurately measured test error over an independently-drawn set of 10,000 data per class. Results for ER are shown in Figure 3, and for VR in Figure 4 for a range of values of σ^2. Ideally, we would like a correlation between training error and test error which displays a clear, single minimum such that minimizing the risk functional over the training set invariably leads to the lowest possible test error.

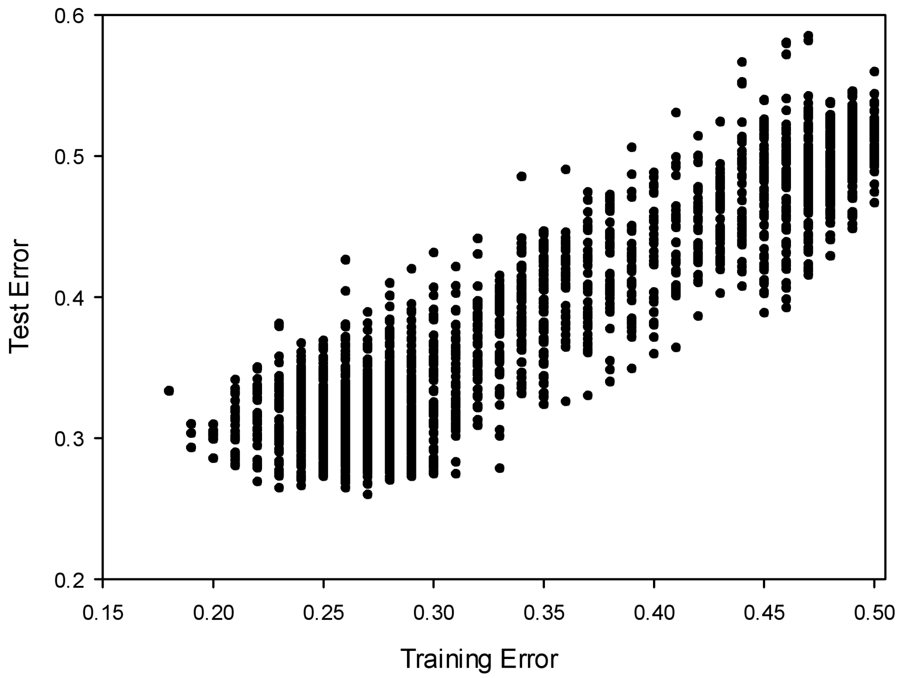

Fig. 3 Correlation between training and test errors for empirical risk. Hastie dataset; 50 training data per class.

The correlation plot for ERM with 50 training data per class in Figure 3 displays vertical striations reinforcing the fact that this is a one-training-error-to-many-possible-test-errors mapping. The minimum test error does not coincide with minimum training error and there is evidence of overfitting by many individuals. Logically, the GP optimization could discover the optimal decision surface by chance which should return the Bayes-optimal test error but the key issue here is that this optimal solution could not be systematically identified using ERM due to its one-to-many nature.

The sequence of plots (Figure 4a to 4d) for VR shows the correlations for different values of σ^2, again for 50 training data per class. For $\sigma^2 = 1 \times 10^{-4}$ much of the striated character of the empirical risk plot in Figure 3 remains implying insufficient smoothing. At the other extreme, Figure 4d does not display a clear minimum. Figure 4c for $\sigma^2 = 0.1$ appears near-optimal with a cloud of points that form a reasonably sharp cusp; training to the minimum value of VR for this value of σ^2 would yield a test error quite close to the Bayes' error for the Hastie dataset of 0.21. Sequences of plots such as those in Figs. 4a to 4d appear to pass through an 'optimum', thereby implying that conventional cross-validation can be used to identify a (near-)optimal value of σ^2. In most of what follows we have 'tuned' σ^2 rather coarsely by only con-

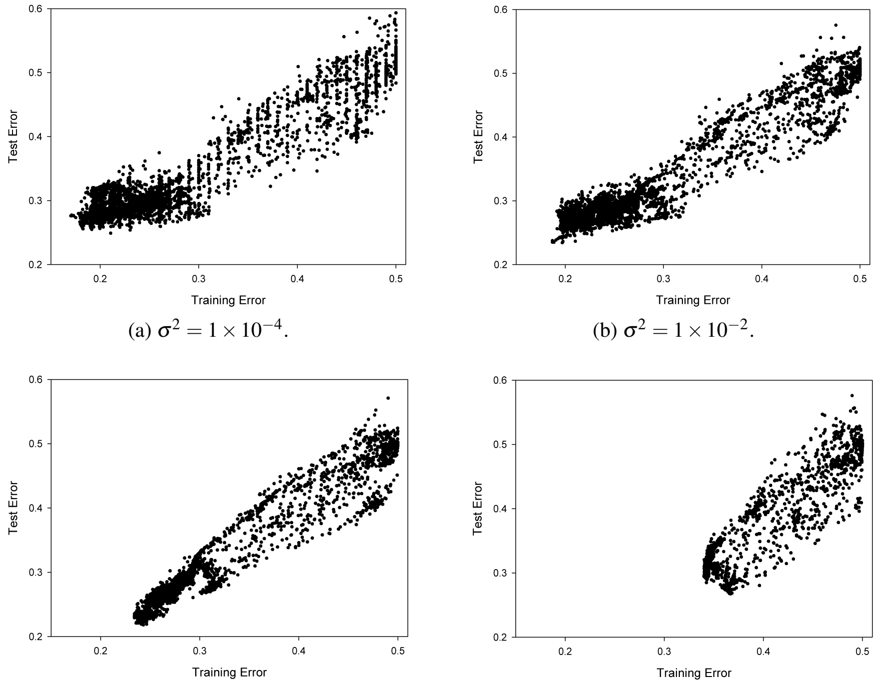

(a) $\sigma^2 = 1 \times 10^{-4}$. (b) $\sigma^2 = 1 \times 10^{-2}$.

(c) $\sigma^2 = 1 \times 10^{-1}$. (d) $\sigma^2 = 1$.

Fig. 4 Correlation between training and test errors for VRM for a range of values of σ^2. Hastie dataset; 50 training data per class.

sidering $\sigma^2 \in \{10^{-3}, 10^{-2}, 10^{-1}, 10^0\}$. A typical but more detailed plot of expected test error over 15 replications against σ^2 is shown in Figure 5 for the WDBC dataset, for the best-performing individuals from the Pareto front. A clear although reassuringly broad minimum is apparent allowing an appropriate determination of σ^2 which justifies the coarse tuning of σ^2 described above. The horizontal dashed line in Figure 5 is the corresponding expected test error for ERM. It is clear that VRM produces a significantly lower error values – we consider statistical testing of differences in errors in the next section.

We have also explored the effect on the above correlations of increasing the number of data in the training set since any useful loss function needs to display the property of consistency – as the number of training data increases, the classifier performance should tend to the Bayes' optimal. In particular, the performance of VRM and ERM should converge with increasing training set size. Figure 6 shows the correlation plots for both VRM and ERM for 500 training data per class drawn from the Hastie dataset, where we have used the same value of $\sigma^2 = 0.1$ that gives (approximately) optimal results for 50 training data per class – see Figure 4c. Figure 6 shows that for these more densely-sampled data, i) the widths of the cigar-shaped clouds of points decrease because the larger number of data better constrains the models, ii) the striated character of the ERM plot (Figure 6b) is no longer apparent for this number

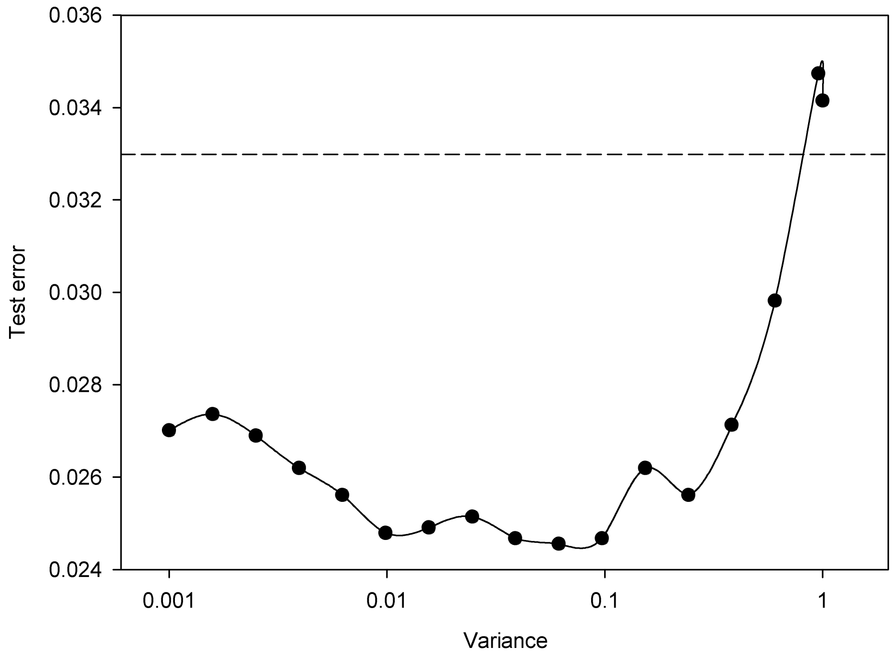

Fig. 5 Expected test error over fifteen data partitions vs. σ^2 for the WDBC dataset. The dashed line is the best mean-of-medians test error for ERM.

of data, and iii) ERM yields a slightly smaller test error (0.2509 vs. 0.2581) although it is questionable whether this is significant. Nonetheless, the more densely-spaced training data require a smaller value of σ^2 than 0.1 to smooth the empirical distribution. (We have made no further attempt to optimize the value of σ^2. Rather we present the result for a sub-optimal value to reinforce the point that the value of σ^2 needs to be tuned to the training dataset at hand. The identical phenomenon is seen in Figures 4 and 5.

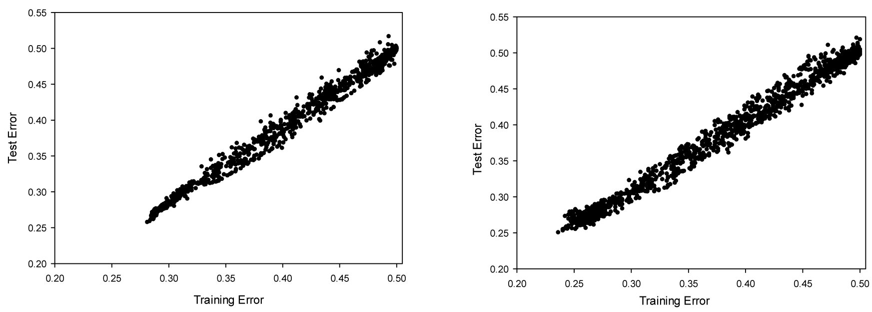

(a) Vicinal Risk Minimization ($\sigma^2 = 0.1$) (b) Empirical Risk Minimization

Fig. 6 Correlations between training and test errors for VRM ($\sigma^2 = 0.1$), and ERM for the Hastie dataset; 1000 training data per class.

4.2 Results over Real and Synthetic Datasets

The average of the median test errors over fifteen repeated partitionings on each dataset are shown in Tables 3 and 4 in the case of VR for optimized values of σ^2
.

- Table 3 shows the results for the individuals with the lowest value of *training* error in the final populations – either empirical or vicinal risk.
- Table 4 shows the results for the individuals with the lowest errors over each test partition taken from the whole Pareto front.

In Tables 3 and 4, the lowest errors are shown bold font. A number of observations can be made from these results.

Firstly, VRM displays the consistently lowest test errors across all datasets in both tables. From a statistical perspective, a Wilcoxon test returns $W^+ = 66$ and $W^- = 0$, where W^+ is the sum of ranks for datasets where ERM delivers a larger test error than VRM [7], and W^- the converse[4]. We obtain a p-value of < 0.01. There is thus very little evidence to support the null hypothesis that the median test errors for ERM and VRM are identical[5].

Second, although minimizing some risk over a training set might be naively presumed to yield the best test error, from the arguments concerning regularization and model selection set-out above, it is clear from comparing values of ERM in Tables 3 and 4, and also VRM across these two tables, that simply minimizing training risk (Table 3) does not deliver the best generalization. A model selection stage over each test partition (Table 4) selects better generalizing models. This procedure is well-established in the conventional machine learning field – see [11, pp. 222-223]. In the multiobjective optimization literature, this procedure is known as *preference articulation* [5]. A statistical comparison along the same lines to that detailed in the paragraph above again yields a p-value of < 0.01, yet again very little evidence to support the null hypothesis that the median errors for the two model selection methods (smallest training error vs. best test partition error) are identical, implying that preference articulation is necessary for the best outcome.

The reason for the superiority of preference articulation is illustrated by Figure 7 which depicts the region around the cusp of the plot of test error versus vicinal risk; the shaded region shows the envelope of correspondences between test error and vicinal risk which can be observed in Figure 4c. Considering first the cusp at the bottom left hand corner of the envelope region in Figure 7. Point ‘B’ is the minimum of vicinal risk whereas point ‘A’ is the minimum of test error. Thus a slightly larger vicinal risk value corresponds to the exact minimum of test error. GP is, of course, a stochastic minimizer with no guarantee of reaching an exact optimum. Therefore consider two plausible points from the Pareto front, ‘C’ and ‘D’ which are proximate to the minimum of vicinal risk (’B’) but not coincident with it – i.e., ‘C’ and ‘D’ are approximate minima of VR. It is clear for this possible outcome that point ‘C’ will

[4] The sum of ranks 1 to 11 = 66.

[5] In this paper we make what may seem to be rather cautious statements about the outcome of hypothesis tests. Hypothesis tests are frequently misinterpreted – see Cohen [6] for a discussion of the technical arguments.

deliver a lower value of test error than 'D' despite having a higher value of vicinal risk. This explains why a separate model selection stage can deliver a smaller value of test error than just minimizing vicinal risk. Notwithstanding this, vicinal risk has a more desirable characteristic than empirical risk – see Figure 3. Further, we show below that VRM produces statistically improved values of test error compared to ERM, as well as having greater repeatability and other properties.

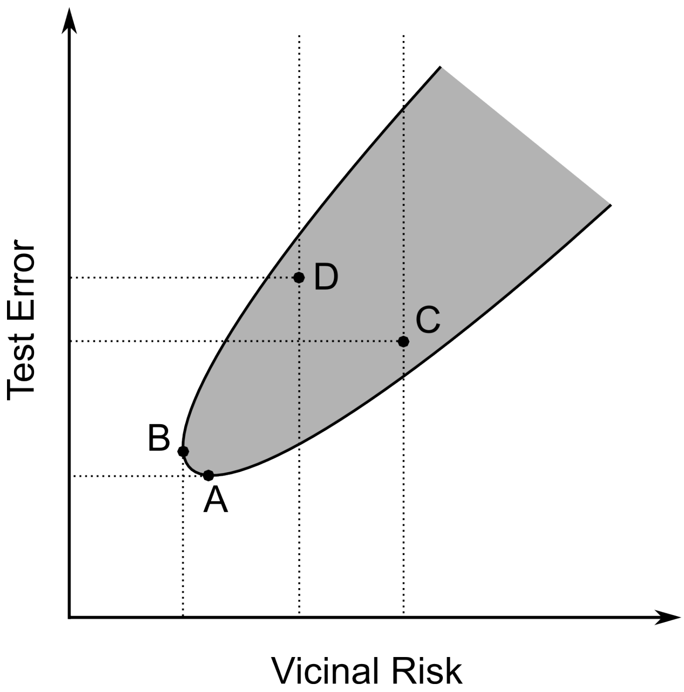

Fig. 7 Illustration of the region around the cusp of the test error/vicinal risk correlation plot showing the justification for a preference articulation stage.

Third, although not shown in Tables 3 and 4, the *variances* of the median test errors averaged over all partitions are quite similar for ERM and VRM for a given dataset, and larger than would be suggested by the variances over any single partition. The explanation is simply that the variance of these values is dominated by the variability due to sampling the multiple training partitions rather than the variablility due to the classifiers. For this reason, the variances of the aggregated test partition errors in Tables 3 and 4 cannot be used for gauging statistical significance although lower averaged median values are still meaningful. We present paired tests below which eliminate this extraneous variability below.

Fourth, the performance of MOGP classifiers trained by ERM is very competitive so the evidence that training with VRM improves upon this is significant. (It is also worth noting that non-separable classification problems have a fundamental lower bound on the attainable on the error rate, the Bayes' error, and it is likely that improvements in performance as this limit is approached are likely to be increasingly difficult to achieve. VRM's improvement on already-good performance is thus noteworthy.)

Table 3 Averaged median test errors for individuals with the best training error; smallest values are shown in bold face.

	ERM	VRM
2-Glass	0.290	**0.284**
BUPA	0.300	**0.292**
PID	0.248	**0.236**
German Credit	0.272	**0.268**
Australian Credit	0.143	**0.134**
Statlog Heart	0.194	**0.165**
WBC	0.0339	**0.0311**
WDBC	0.0391	**0.0317**
Ripley	0.0877	**0.0607**
Hastie	0.302	**0.286**
10D-G	0.417	**0.391**

Table 4 Averaged median test errors for the best individuals on the Pareto front; smallest values are shown in bold face.

	ERM	VRM
2-Glass	0.247	**0.233**
BUPA	0.266	**0.259**
PID	0.232	**0.221**
German Credit	0.257	**0.256**
Australian Credit	0.130	**0.125**
Statlog Heart	0.167	**0.150**
WBC	0.0289	**0.0257**
WDBC	0.0330	**0.0248**
Ripley	0.0720	**0.0523**
Hastie	0.268	**0.245**
10D-G	0.356	**0.348**

Within each dataset, we can compare VR (for optimized σ^2) with empirical risk using the Wilcoxon test. Results over the fifteen data partitions are summarized in Table 5 (selected individuals with the lowest training error), and Table 6 (selected individuals with lowest test partition error). W^+ is the sum of ranks for partitions for which ERM produces larger test error than VRM, and W^- the converse. As before, we have taken the median test error over 30 independently-initialized runs as representative of the test error over each of the fifteen partitions.

For most datasets, there is little evidence to support the null hypothesis that training by ERM and VRM produce the same averaged median test error, the only exceptions being the result for 2D-Glass in Table 5 and for German Credit in Table 6. This could be a manifestation of the probabilistic nature of hypothesis testing – perform enough tests and eventually one will yield an erroneous result due to the non-zero probability of type II error. Nonetheless, taking the results at face value, VRM gener-

Table 5 Wilcoxon's test comparing 0/1 loss and VRM within each dataset; selected individuals with the lowest training set error

Dataset	Optimal σ^2	W-score	p-value
2D-Glass	10^{-2}	$W^+ = 61.5W^- = 29.5$	$= 0.26$
BUPA	10^{-3}	$W^+ = 92.5, W^- = 12.5$	< 0.02
PID	10^{0}	$W^+ = 91.5, W^- = 13.5$	< 0.02
German	10^{-1}	$W^+ = 105.5, W^- = 14.5$	< 0.01
Australian	10^{0}	$W^+ = 105, W^- = 0$	< 0.01
Statlog Heart	10^{0}	$W^+ = 91.5, W^- = 13.5$	< 0.02
WBC	10^{-1}	$W^+ = 42, W^- = 3$	≤ 0.02
WDBC	10^{-1}	$W^+ = 120, W^- = 0$	< 0.01
Ripley	10^{-1}	$W^+ = 75, W^- = 3$	< 0.01
Hastie	10^{-1}	$W^+ = 84.5, W^- = 20.5$	< 0.05
10D-G	10^{0}	$W^+ = 97.5, W^- = 7.5$	< 0.01

Table 6 Wilcoxon's test comparing 0/1 loss and VRM within each dataset; selected individuals with the lowest test partition error on the Pareto front.

Dataset	Optimal σ^2	W-score	p-value
2D-Glass	10^{-2}	$W^+ = 91, W^- = 0$	< 0.01
BUPA	10^{-3}	$W^+ = 105, W^- = 0$	<0.01
PID	10^{-1}	$W^+ = 91, W^- = 0$	< 0.01
German	10^{-1}	$W^+ = 52, W^- = 26$	$= 0.30$
Australian	10^{0}	$W^+ = 91, W^- = 0$	< 0.01
Statlog Heart	10^{0}	$W^+ = 105, W^- = 0$	< 0.01
WBC	10^{-1}	$W^+ = 69, W^- = 9$	≤ 0.02
WDBC	10^{-1}	$W^+ = 120, W^- = 0$	< 0.01
Ripley	10^{-1}	$W^+ = 76, W^- = 2$	< 0.01
Hastie	10^{-3}	$W^+ = 91, W^- = 0$	< 0.01
10D-G	10^{-1}	$W^+ = 66, W^- = 12$	< 0.05

ally delivers superior results and, at very worst, two results which are not statistically different. In no case is ERM superior to VRM. (It should also be noted that 2D-Glass VRM vs. ERM produced 8 'wins' for VRM and 5 'losses' out of 15 pairwise comparisons; for the German Credit dataset, the corresponding figures are 8 'wins' and 4 'losses'. That is, VRM still performs better on raw count.)

From Tables 5 and 6, it is obvious that the optimal value of σ^2 and the apparent superiority of VRM both vary by dataset which is expected as each problem has different characteristics.

4.3 Stability of Training

Although we have demonstrated above that VRM is able to produce a superior *median* test error, a median is a statistic that can potentially hide a number of important details. In particular, what are the comparative *spreads* of test error for multiple runs, or alternatively, what is the probability that training with VRM will produce a better outcome than training with ERM? We have performed multiple runs using the same test partitions but with different initial populations and plotted the results as a histogram. We present two histograms of test error for the real WDBC dataset, for two randomly selected data partitions in Figure 8, and two corresponding histograms for the synthetic Ripley dataset in Figure 9.

It can be seen from Figures 8 and 9 that the histograms for VRM are more compact with modes at lower values of test error than for ERM, indicating that VRM training is, on average, more stable and more likely to deliver a lower test error.

5 Discussion

In essence, what we are doing in the VRM approach is to form a 'better' approximation of the underlying class-conditioned densities by smoothing-out the set of discrete samples in the training set. In this sense, σ^2 is another kind of regularizing parameter which needs to be adjusted to obtain best results. Similar although differently-motivated approaches have previously been employed with multi-layer perceptron (MLP) neural networks. For example, Holmström and Koistenen [12] obtained improved generalization performance by adding Gaussian-distributed noise to the training set in an ad hoc manner. Karystinos and Pados [14] employed a much more elaborate approach of modeling the distribution of input variables and then drawing a large, similarly-distributed training set which yielded improved performance.

Placing Gaussian kernels over a training data is Parzen window density estimation [8] where the width of the kernels is a smoothing parameter which has to be tuned, typically by cross-validation. Under Parzen window estimation, the probability density function (PDF) of each class is approximated by a (normalized) summation of Gaussian kernels. Assuming a two-class problem ('A' vs. 'B') and the approximation of the class-conditioned PDF for class 'A' is given by $\tilde{p}_A(\mathbf{x}|A)$, the risk associated with misclassifying a pattern drawn from 'A' is given by:

$$\mathscr{R}_A = \int_{\Omega} \tilde{p}_A(\mathbf{x}|A)d\mathbf{x} \tag{8}$$

where $\mathbf{x} \in \mathbb{R}^N$ and the region of integration, Ω is the portion of N-dimensional pattern space to the right of the decision surface in Figure 10. A similar argument holds for class 'B' which can be approximated by $\tilde{p}_B(\mathbf{x}|B)$ and where the integral defining $\mathscr{R}_B$ is taken over the region of space in Figure 10 to the *left* of the decision boundary, namely the complement of Ω. The overall probability of error, $P(error)$ is given by a weighted sum of $\mathscr{R}_A$ and $\mathscr{R}_B$:

$$P(error) = \kappa_{AB}P(A)\mathscr{R}_A + \kappa_{BA}P(B)\mathscr{R}_B \tag{9}$$

where κ_{ij} is the cost of misclassifying a pattern from class i as belonging to class j which we can, without loss of generality, assume to be unity. $P(A)$ and $P(B)$ are the prior probabilities of classes 'A' and 'B', respectively. By selection of an appropriate decision surface (i.e., by classifier training), (9) can be minimized to yield (close to) the Bayes' optimal error. Since $\tilde{p}_k(\mathbf{x}|k)$, $k \in \{A, B\}$ are approximated by a (normalized) sum of Gaussian kernels, one for each training pattern, it follows that minimizing (9) is equivalent to minimizing the vicinal risk under the assumption of a meaningful discriminant $g()$ that separates the majority of points in one class

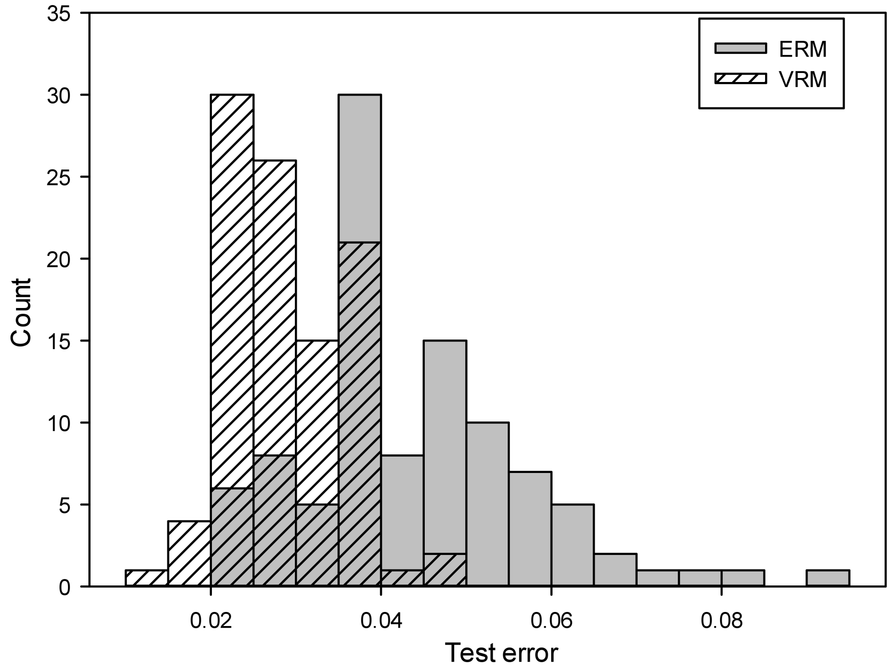

(a) Partition #1

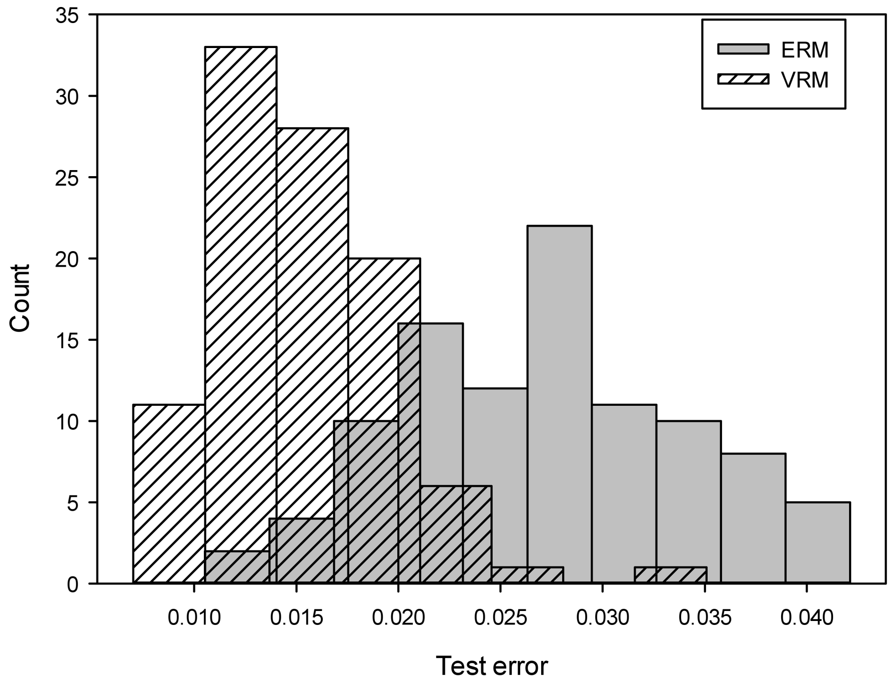

(b) Partition #8

Fig. 8 Histograms of test error for two randomly-selected partitions of the WDBC dataset, for trees trained by both VRM and ERM.

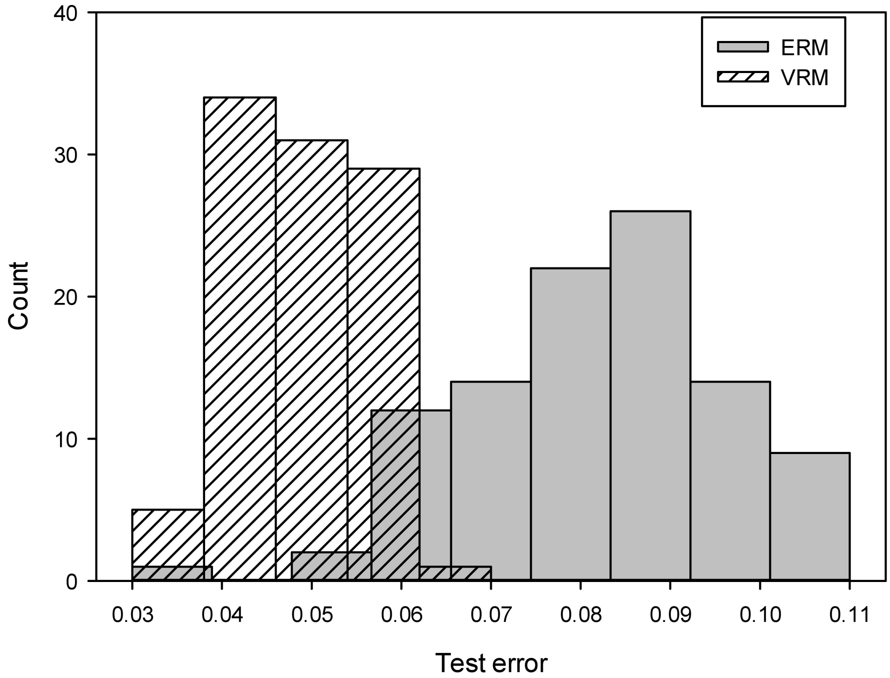

(a) Partition #3

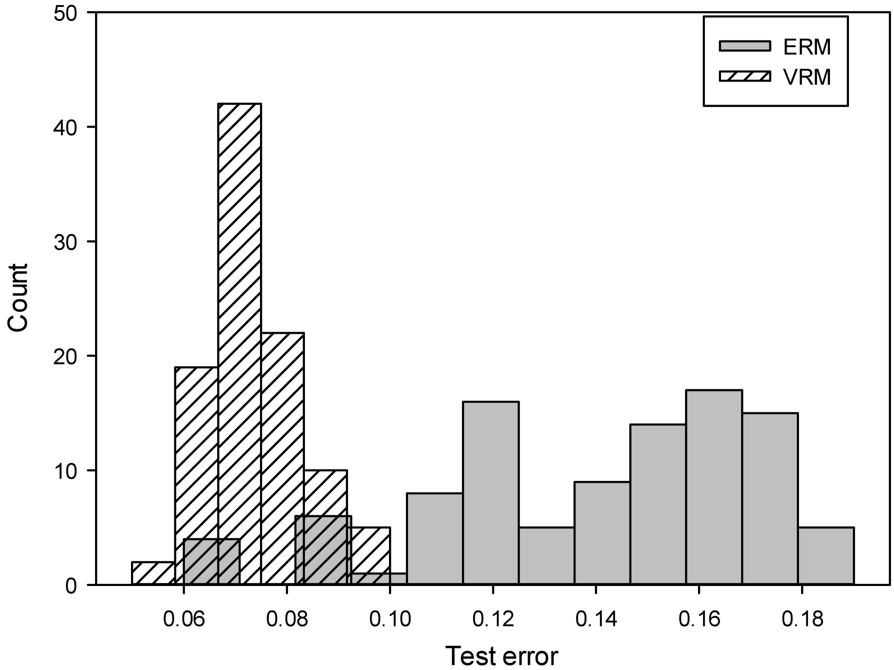

(b) Partition #11

Fig. 9 Histograms of test error for two randomly-selected partitions of the Ripley dataset, for trees trained by both VRM and ERM.

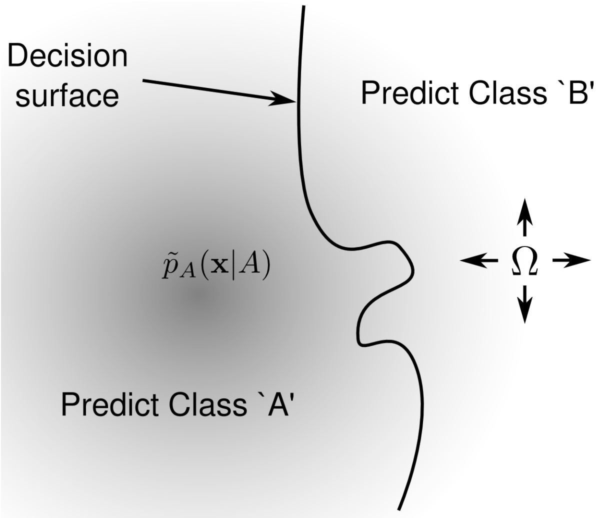

Fig. 10 Illustration of the domain of integration over pattern space to calculate risks.

such that $g(\mathbf{x}) - t > 0$ and the majority of the points in the other class such that $g(\mathbf{x}) - t < 0$. VRM can thus be directly related to minimizing the overall probability of error. The significant advantage of the formulation presented in this paper is that the class-conditioned risks $\mathscr{R}_{A,B}$ (8) are evaluated in the 1D decision space rather than in N-dimensional pattern space over, typically, a region of integration defined by a highly non-linear decision surface. (Indeed, in our experience, GP classifiers can frequently generate disjoint decision regions in pattern space.)

As to why vicinal risk does not exhibit *perfect* correlation with test error (Section 4.1), obviously the (implicitly) assumed forms for $\tilde{p}_{A,B}(\mathbf{x}|A,B)$ are approximations and therefore incur some error. Nonetheless, VRM is able to consistently guide the optimization to consistently superior regions of the solution space and is thus a demonstrable improvement over ERM.

In the light of the motivation for VRM in Section 1 and the experimental results in Section 4, it is worth reiterating the contribution of this paper. From Figure 1, it is clear that by minimizing empirical risk, it is quite possible to locate the superior discriminant g_2 although is is also equally likely to locate the inferior g_1 instead. To reiterate the key issue: as illustrated in Figure 1, training by ERM cannot distinguish between good and bad solutions. We do not claim that VRM will *always* produce superior solutions to ERM. Indeed, it is possible that the ill-posed ERM may well fortuitously find a solution which as as good as the VRM solution. The role of VRM, however, is to *stabilize* the training process. We have demonstrated that VRM has a consistently higher probability of producing a superior result which, in a compute-intensive scenario such as GP, is a significant advantage. Rather than the commonly-used practice of making multiple GP runs using ERM and selecting the best, VRM has a higher probability of yielding a good solution in a single run.

Finally, implementation of VRM training used here is very simple and amounts to drawing an augmented training set, in advance, from the Parzen density estimate of the original data. For the case of small datasets where the ill-posedness due to the 0/1 loss is most problematic, the use of Monte Carlo integration is not a significant burden although we can envisage an 'early jump-out' technique to speed-up the computations. The integral for the i-th pattern is evaluated by counting the fraction of the augmented samples from this pattern that falls on the wrong side of the decision surface – see Figure 2. Only training patterns proximate to the decision surface are likely to be misclassified – patterns a long way from the decision boundary will never be misclassified. Therefore, if the first n Monte Carlo samples from the i-th pattern are all correctly classified, there is a probably little value in considering the remaining samples; to some confidence level, we can thus 'jump-out' the integral evaluation early for the i-th pattern since it is likely to contribute nothing to the vicinal risk. This is an area for future investigation.

6 Conclusions

In this paper we have introduced and motivated vicinal risk minimization (VRM) for training genetic programming classifiers. VRM is formulated by placing a Gaussian kernel on each training datum in pattern space and propagating the resulting errors on the decision into the 1D decision space. Minimizing vicinal risk over the training set is shown to be equivalent to approximately minimizing the overall probability of error for the problem in a Bayesian setting. VRM is shown to be far better correlated with test error than empirical risk minimization (ERM), that is, minimizing vicinal risk leads to consistently improved classifier generalization. The widths of the Gaussian kernels can be straightforwardly chosen by cross-validation.

We present statistical comparisons between ERM and VRM which indicate there is very little evidence to support the null hypotheses that the two loss functions perform identically. VRM is shown not to completely remove the need for a model selection stage over the Pareto front of equivalent solutions although there is good evidence that it guides the evolutionary optimization to improved solutions.

Acknowledgements The authors would like to thank Yilong Cao and Richard Everson for valuable discussions.

References

1. Amil, N.M., Bredeche, N., Gagné, C., Gelly, S., Schoenauer, M., Teytaud, O.: A statistical learning perspective of genetic programming. In: 12^{th} European Conference on Genetic Programming (EuroGP 2009), pp. 327–338. Tübingen, Germany (2009)
2. Borges, C.E., Alonso, C.L., Montaña, J.L.: Model selection in genetic programming. In: 12^{th} Annual Conference on Genetic and Evolutionary Computation (GECCO 2010), pp. 985–986. Portland, OR (2010)
3. Chapelle, O., Weston, J., Bottou, L., Vapnik, V.: Vicinal risk minimization. In: Advances in Neural Information Processing Systems 13 (NIPS 2000), pp. 416–422. Denver, CO (2000)
4. Cherkassky, V., Mulier, F.M.: Learning from Data: Concepts, Theory and Methods, 2^{nd} edn. Wiley-IEEE Press (2007)

5. Coello, C.A.C., Lamont, G.B.: Applications of Multi-Objective Evolutionary Algorithms, vol. 1. World Scientific, Singapore (2004)
6. Cohen, J.: The earth is round ($p < .05$). Am. Psychol. **49**(12), 997–1003 (1994)
7. Demšar, J.: Statistical comparisons of classifiers over multiple data sets. J. Mach. Learn. Res. **7**, 1–30 (2006)
8. Duda, R.O., Hart, P.E., Stork, D.G.: Pattern Recognition, 2nd edn. John Wiley & Sons, New York (2001)
9. Ekárt, A., Németh, S.Z.: Selection based on the Pareto nondomination criterion for controlling code growth in genetic programming. Genet. Program. Evol. M. **2**(1), 61–73 (2001)
10. Frank, A., Asuncion, A.: UCI Machine Learning Repository. University of California, Irvine, School of Information and Computer Sciences (2010). URL `http://archive.ics.uci.edu/ml`
11. Hastie, T., Tibshirani, R., Friedman, J.: The Elements of Statistical Learning: Data Mining, Inference, and Prediction, 2^{nd} edn. Springer-Verlag (2009)
12. Holmström, L., Koistinen, P.: Using additive noise in back-propagation training. IEEE T. Neural. Networ. **3**(1), 24–38 (1992)
13. Iba, H., de Garis., H., Sato, T.: Genetic programming using a minimum description length principle. In: Advances in Genetic Programming, pp. 265–284. MIT Press (1994)
14. Karystinos, G.N., Pados, D.A.: On overfitting, generalization, and randomly expanded training sets. IEEE T. Neural. Networ. **11**(5), 1050–1057 (2000)
15. Kumar, R., Rockett, P.I.: Improved sampling of the Pareto-front in multiobjective genetic optimizations by steady-state evolution: A Pareto converging genetic algorithm. Evol. Comput. **10**(3), 283–314 (2002)
16. Nadeau, C., Bengio, Y.: Inference for the generalization error. Mach. Learn. **52**(3), 239–281 (2003)
17. Polak, E.: Optimization: Algorithms and Consistent Approximations. Springer, New York (1997)
18. Poli, R., Langdon, W.B., McPhee, N.F.: A Field Guide to Genetic Programming. Published via `http://lulu.com` and freely available at `http://www.gp-field-guide.org.uk` (2008)
19. Ripley, B.D.: Neural networks and related methods for classification. J. Roy. Stat. Soc. B Met. **56**(3), 409–456 (1994)
20. Rissanen, J.: Modeling by shortest data description. Automatica **14**(5), 465–471 (1978)
21. Robert, C.P., Casella, G.: Monte Carlo Statistical Methods, 2^{nd} edn. Springer-Verlag, New York (2005)
22. Silva, S., Dignum, S., Vanneschi, L.: Operator equalisation for bloat free genetic programming and a survey of bloat control methods. Genet. Program. Evol. M. **13**(2), 197–238 (2012)
23. Soares, C.: Is the UCI repository useful for data mining? In: 11^{th} Portuguese Conference on Artificial Intelligence (EPIA 2003), pp. 209–223. Beja, Portugal (2003)
24. Tikhonov, A.N., Arsenin, V.Y.: Solutions of Ill Posed Problems. V.H. Winston, Washington, D.C (1977)
25. Vapnik, V.N.: The Nature of Statistical Learning Theory, 2^{nd} edn. Springer, New York (2000)
26. Zhang, Y., Rockett, P.: A comparison of three evolutionary strategies for multiobjective genetic programming. Artif. Intell. Rev. **27**(2-3), 149–163 (2007)
27. Zhang, Y., Rockett, P.I.: A generic optimising feature extraction method using multiobjective genetic programming. Appl. Soft Comput. **11**(1), 1087–1097 (2011)